

VACUUM CARBOTHERMIC REDUCTION OF BAUXITE COMPONENTS: A THERMODYNAMIC STUDY

M. Halmann¹, M. Epstein², and A. Steinfeld³

¹Department of Environmental Sciences and Energy Research, Weizmann Institute of Science, Rehovot, Israel

²Weizmann Institute of Science, Solar Research Unit, Rehovot, Israel

³Department of Mechanical and Process Engineering, ETH Zurich, Zurich, Switzerland, and Solar Technology Laboratory, Paul Scherrer Institute, Villigen, Switzerland

The possibility of direct vacuum carbothermic reduction of bauxite minerals to metallic aluminum at a temperature of 1400–1500 K and a pressure of 10^{-7} bar is examined by thermochemical equilibrium calculations on $\text{AlO}(\text{OH})$ (boehmite and diaspore) and $\text{Al}(\text{OH})_3$ (gibbsite) in the absence and presence of SiO_2 , TiO_2 , and $\text{FeO}(\text{OH})$. Carbon monoxide and hydrogen coproduced by the reaction may be used as combustion fuel or further processed to liquid hydrocarbons. The vacuum carbothermic reduction of iron-rich calcined bauxite was studied for $\text{Al}_2\text{O}_3\text{--Fe}_2\text{O}_3\text{--C}$ mixtures at 10^{-4} , 10^{-5} , and 10^{-6} bar, indicating narrow temperature ranges at which the equilibrium for the release of gaseous Al is favored relative to gaseous Fe. Alternatively, for iron-rich bauxite, a preliminary step of iron-removal would be necessary. The proposed process could potentially decrease energy consumption and greenhouse gas emissions, and avoid the production of “red mud.”

Keywords: alumina, aluminum, bauxite, carbothermic reduction, thermodynamics, vacuum

INTRODUCTION

Current aluminum production is based on two main stages: (a) the Bayer process for producing Al_2O_3 from a mixture of minerals composing the deposits of bauxite, followed by (b) the Hall-Héroult process for electrolytically converting Al_2O_3 to Al. The major Al-containing components of bauxite are gibbsite (hydrargillite) $\gamma\text{-Al}(\text{OH})_3$ (or $\text{Al}_2\text{O}_3\cdot 3\text{H}_2\text{O}$), boehmite $\gamma\text{-AlO}(\text{OH})$, and diaspore $\alpha\text{-AlO}(\text{OH})$ (or $\text{Al}_2\text{O}_3\cdot\text{H}_2\text{O}$), often accompanied by the iron mineral goethite $\text{FeO}(\text{OH})$, as well as aluminosilicates and titanium minerals. Both the Bayer process and the Hall-Héroult electrolytic process are characterized by their high-energy consumption (0.045 GJ/kg Al) and the associated high specific $\text{CO}_2\text{-equiv}$ emissions (4.9–7.4 kg $\text{CO}_2\text{-equiv}/\text{kg Al}$) (Choate and Green, 2006; International Aluminum Institute, 2009). The Bayer process often requires a stage of mineral beneficiation, which

Address correspondence to M. Halmann, Weizmann Institute of Science, Department of Environmental Sciences and Energy Research, Rehovot 76100, Israel. E-mail: m.halmann@weizmann.ac.il

involves the removal of fines and the separation of iron oxides by hydrochloric acid leaching (Reddy, Mishra, and Banerjee 1999; Gülfen, Gülfen, and Ayden 2006) or by froth flotation and magnetic separation (Renata et al. 2009), and further coproduces a strong alkaline waste (red mud). A possible alternative route to metallic aluminum could be the high-temperature carbothermal reduction of the aluminum minerals. In previous work, the carbothermal reduction of Al_2O_3 , was performed using concentrated solar energy (Murray, Steinfeld, and Fletcher 1995; Murray 1999, 2001; Kruesi et al. 2011) or induction furnace heating (Halmann, Frei, and Steinfeld 2007) as the sources of high-temperature process heat, thus significantly reducing the discharge of greenhouse gases and other pollutants derived from the combustion of fossil fuels. In a study of the vacuum carbothermal processing of low-iron bauxite from the Republic of Komi in the Ural region of Russia, a mixture of calcined bauxite and charcoal (80:20 by weight) heated up to 1600°C in a corundum (α -alumina) vacuum reactor tube resulted in the condensation of β -SiC, $\text{Al}_4\text{O}_4\text{C}$, Al, Al_4C_3 , and α -alumina on the cold wall of the reactor, and in a residue of α -alumina, TiC, and FeO in the hot zone of the reactor (Goldin et al. 1998). The initial vacuum of the reactor was reported to be down to 10^{-3} Pa (10^{-8} bar, or 7.5×10^{-6} torr), but during the heat treatment, the reaction resulted in the copious release of CO, $\text{Al}_2\text{O}(\text{g})$, and $\text{SiO}(\text{g})$ with a surge in gas pressure. The production of primary Al-Si alloys was studied by the vacuum carbothermal reduction of floated bauxite tailings containing mainly Al_2O_3 , SiO_2 , and Fe_2O_3 (about 44, 26, and 10.5 wt.%, respectively), using bituminite as a reductant, in a graphite furnace at pressures down to 0.1 MPa (10^{-9} bar) and temperatures up to 2000°C , resulting in the formation of an Al-Si-Fe alloy, as well as carbides and elementary Al and Si. The process was tested both on a laboratory and pilot-plant scale. The proposed mechanism involves the intermediate formation and decomposition of carbides, in which the presence of Fe has a catalytic effect (Yang et al. 2010).

In the present study, the thermodynamics of the carbothermal reduction of low-iron bauxites is examined as a possible direct route from bauxite to aluminum, by calculating the equilibrium compositions as a function of temperature of either separately $\text{Al}(\text{OH})_3$ or $\text{AlO}(\text{OH})$ with the stoichiometric amounts of carbon, or of the reactions of $\text{AlO}(\text{OH})$ and carbon with small amounts of $\text{FeO}(\text{OH})$, or SiO_2 , or TiO_2 . An example of a similar calculation for high-iron bauxite is made on the reported composition of the diaspore bauxite deposits in the Mt. Parnassus region of Greece (Aluminum of Greece). In addition, the vacuum carbothermic reduction of iron-rich calcined bauxite was studied for Al_2O_3 - Fe_2O_3 -C mixtures at 10^{-4} , 10^{-5} , and 10^{-6} bar, in order to elucidate possible selectivity in the production of gaseous Al relative to gaseous Fe. Thermochemical equilibrium computations were carried out using the FactSage software (Factsage). The total enthalpy of the reaction was calculated in two steps. Reaction enthalpies at atmospheric pressure (1 bar) were derived using the data of the NIST webbook (NIST). The theoretical work input for isothermal expansion of the product gases from atmospheric pressure to a vacuum pressure p is $nRT \ln p$, where n is the increase in the number of gas moles formed per mole of the metal oxide, $R = 8.414 \times 10^{-3}$ kJ $\text{K}^{-1} \text{mol}^{-1}$ is the gas constant, and T is the absolute temperature. Reaction onset temperatures were taken at about 0.001% conversion of the metal oxides to the metals.

THERMODYNAMIC ANALYSIS

The System $\text{Al}(\text{OH})_3 + 3\text{C}$ at 10^{-7} Bar

The variation of the equilibrium composition with temperature for the carbothermic reduction of gibbsite, with initially $\text{Al}(\text{OH})_3 + 3\text{C}$ is shown in Figure 1. The onset temperature of $\text{Al}(\text{g})$ formation at 10^{-7} bar is 1170 K. At 1400 K and 10^{-7} bar the equilibrium becomes



All the carbon consumed in the reaction would be converted into CO. By partial water-gas shift, 1/2 of the CO may be converted into H_2 to produce together with the directly formed H_2 a syngas mixture with the molar ratio $\text{H}_2/\text{CO}=2$, suitable either for methanol synthesis or for the Fischer-Tropsch reaction to hydrocarbons.

The System $\text{AlO}(\text{OH}) + 2\text{C}$ at 10^{-7} Bar

The equilibrium composition versus temperature is shown in Figure 2. The onset temperature of $\text{Al}(\text{g})$ formation by carbothermic reduction of boehmite at 10^{-7} bar is 1200 K. At 1400 K and 10^{-7} bar the equilibrium becomes



The System $\text{AlO}(\text{OH}) + 0.1\text{TiO}_2 + 2.2\text{C}$ at 10^{-7} Bar

The equilibrium composition versus temperature is shown in Figure 3. The onset temperatures of $\text{Al}(\text{g})$ formation at 10^{-7} bar is 1230 K. At 1400 K and

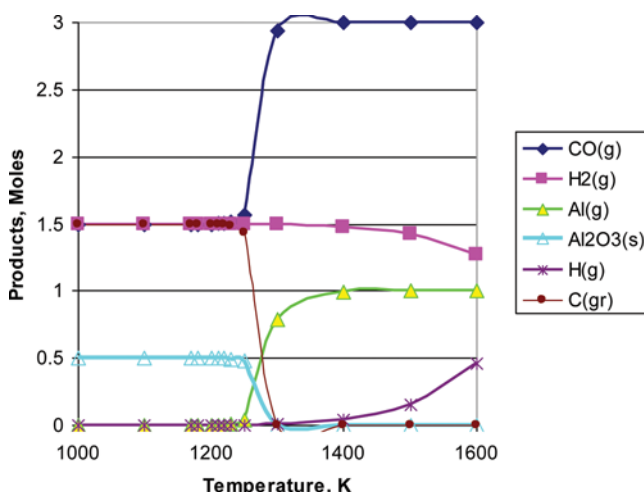


Figure 1 Temperature dependence for the system $\text{Al}(\text{OH})_3 + 3\text{C}$ at 10^{-7} bar (color figure available online).

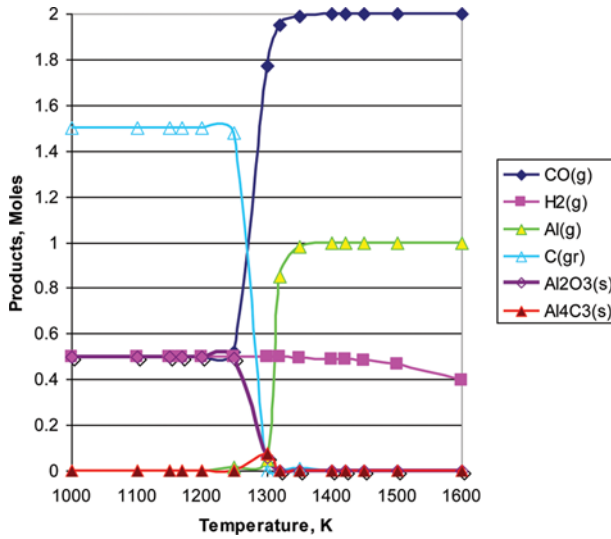


Figure 2 Temperature dependence for the system $\text{AlO(OH)} + 2\text{C}$ at 10^{-7} bar (color figure available online).

10^{-7} bar the equilibrium becomes:

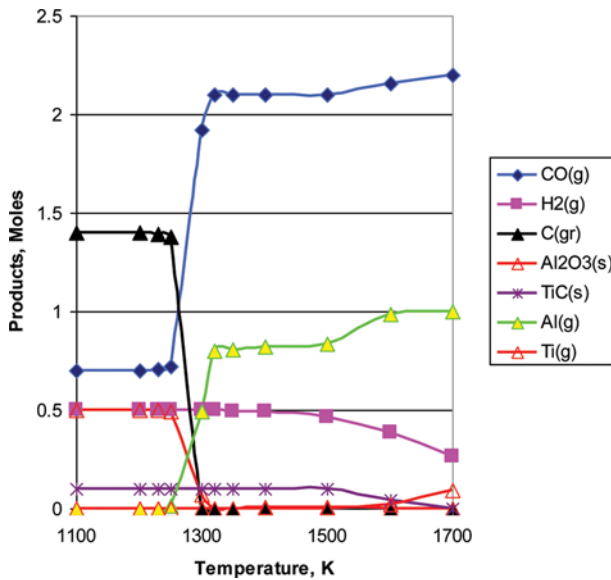
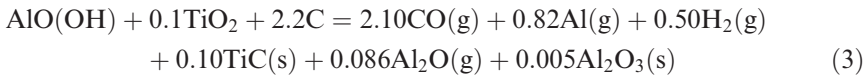
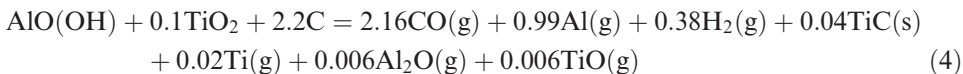


Figure 3 Temperature dependence for the system $\text{AlO(OH)} + 0.1\text{TiO}_2 + 2.2\text{C}$ at 10^{-7} bar (color figure available online).

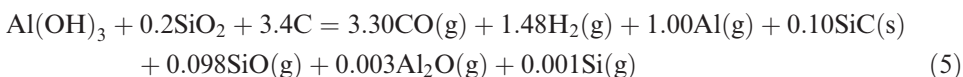
At 1600 K, the equilibrium product distribution becomes:



In the temperature range of 1350–1600 K there is no appreciable interference of gaseous titanium on the formation of gaseous aluminum.

The System $\text{Al(OH)}_3 + 0.2\text{SiO}_2 + 3.4\text{C}$ at 10^{-7} Bar

The equilibrium composition versus temperature is shown in Figure 4. The onset temperatures of Al(g) formation at 10^{-7} bar is 1200 K, as shown in Figure 4. At 1400 K and 10^{-7} bar, the equilibrium reaction can be represented by:



At this temperature, there is no significant interference of Si(g) on Al(g) production.

The System $\text{AlO(OH)} + 0.2\text{SiO}_2 + 2.4\text{C}$ at 10^{-7} Bar

This calculation was made for the carbothermal reduction of a low-iron bauxite, with the average composition after calcinations of 75.34 wt% $\gamma\text{-AlO(OH)}$ and 15.3 wt% SiO_2 , or a molar ratio of $\text{SiO}_2/\text{AlO(OH)} = 0.20$ (Goldin et al. 1998).

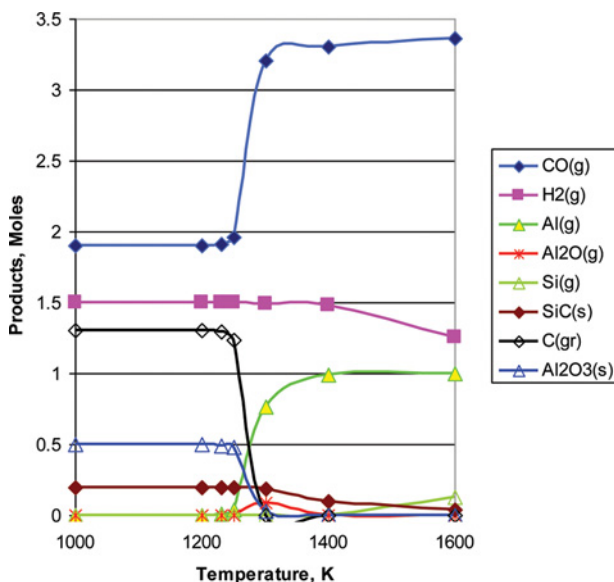
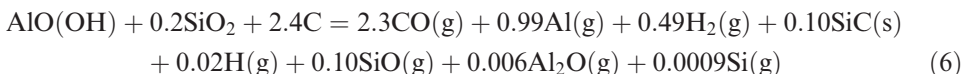


Figure 4 Temperature dependence for the system $\text{Al(OH)}_3 + 0.2\text{SiO}_2 + 3.4\text{C}$ at 10^{-7} bar (color figure available online).

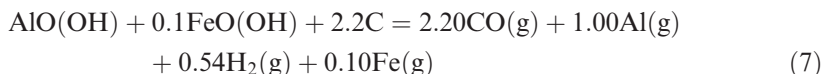
The equilibrium composition versus temperature is shown in Figure 5. The onset temperatures of Al(g) formation at 10^{-7} bar is 1200 K. At 1400 K and 10^{-7} bar the equilibrium becomes



At 1400 K there is no interference of Si(g) on the production of Al(g), which however becomes significant above 1500 K.

The System $\text{AlO(OH)} + 0.1\text{FeO(OH)} + 2.2\text{C}$ at 10^{-7} Bar

This system, shown in Figure 6, was tested as an example of bauxite with relatively low iron content (Goldin et al. 1998). The onset temperatures of both Al(g) and Fe(g) formation at 10^{-7} bar are about 1200 K. At 1400 K and 10^{-7} bar the equilibrium becomes



The molar ratio Al/Fe = 1:0.1 in the gaseous mixture at 1400 K is the same as in the original reactant mixture.

The System $\text{AlO(OH)} + 0.28\text{FeO(OH)} + 2.56\text{C}$ at 10^{-7} Bar

This system was tested as an example of bauxite with a high iron content, such as with 50%–60% $\text{Al}_2\text{O}_3 \cdot \text{H}_2\text{O}$, 18%–25% Fe_2O_3 , 1%–6% SiO_2 , 2%–6% TiO_2 ,

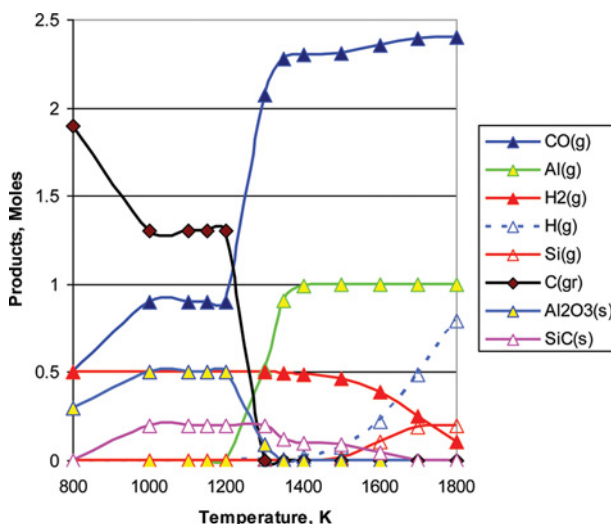


Figure 5 Temperature dependence for the system $\text{AlO(OH)} + 0.2\text{SiO}_2 + 2.4\text{C}$ at 10^{-7} bar (color figure available online).

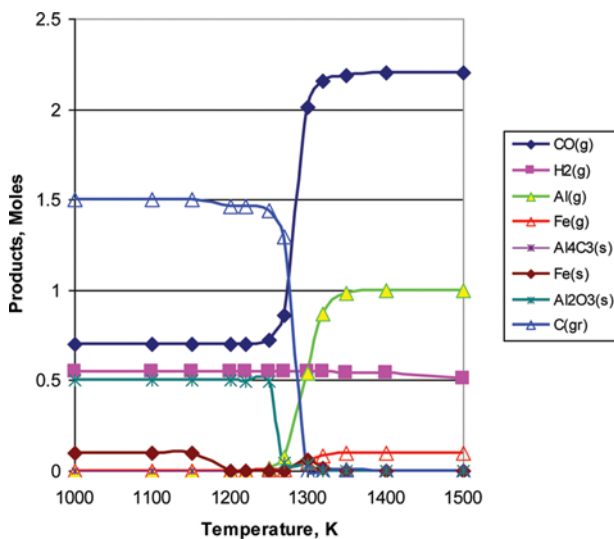


Figure 6 Temperature dependence for the system $\text{AlO}(\text{OH}) + 0.1\text{FeO}(\text{OH}) + 2.2\text{C}$ at 10^{-7} bar (color figure available online).

and 1%–3% CaCO_3 (weight-%) (Aluminum of Greece). The equilibrium composition versus temperature is shown in Figure 7. The molar ratio of $\text{Fe}_2\text{O}_3/\text{Al}_2\text{O}_3 \cdot \text{H}_2\text{O}$ is thus 0.28. The onset temperature of $\text{Fe}(\text{g})$ and $\text{Al}(\text{g})$ formation are 1100 K and

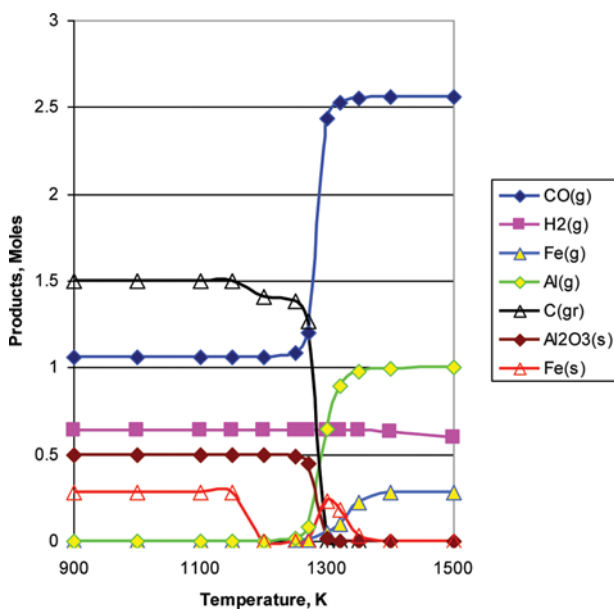
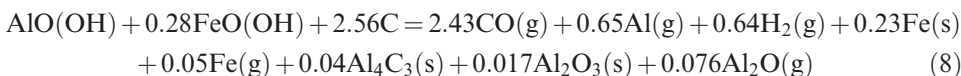


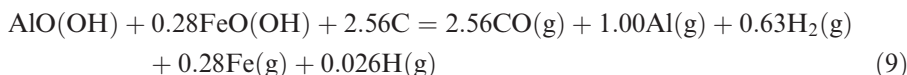
Figure 7 Temperature dependence for the system $\text{AlO}(\text{OH}) + 0.28\text{FeO}(\text{OH}) + 2.56\text{C}$ at 10^{-7} bar (color figure available online).

1200 K, respectively. At 1300 K, the equilibrium reaction is:



At 1300 K and 10^{-7} bar, at which the equilibrium is $\text{Fe(g)}/\text{Al(g)} = 0.077$, there could thus be a window of opportunity, in which most of the iron is in the solid form, and only a small fraction is gaseous. With careful temperature control, it may theoretically be possible to obtain Al(g) almost free of iron, if the kinetics will also be favorable.

At 1400 K, the reaction can be represented by



Therefore at this temperature there is no separation of Al(g) from Fe(g), and it would not be possible to obtain pure aluminum free of iron. However, this process could possibly be useful for the direct production of Al-Fe alloys.

The System $\text{Al}_2\text{O}_3 + 0.23\text{Fe}_2\text{O}_3 + 3.7\text{C}$ at 10^{-4} , 10^{-5} , and 10^{-6} Bar

Possible ways of separating aluminum from iron by carbothermic reduction of calcined bauxite are explored. The calculations were made for an alumina-hematite mixture representative of Greek bauxite (see Table 1), containing 60.2 wt% Al_2O_3 and 21.7 wt% Fe_2O_3 , or a $\text{Fe}_2\text{O}_3/\text{Al}_2\text{O}_3$ molar ratio of 0.23. The equilibrium compositions versus temperature for the above systems at 10^{-4} , 10^{-5} , and 10^{-6} bar are shown in Figures 8–10. At all these pressures there seem to be narrow temperature ranges at which the gaseous Al is favored over gaseous Fe, while at that temperature iron is still mainly in the form of Fe(s) or Fe_3C (liquid). At 1600 K and 10^{-4} bar, the equilibrium formed is:

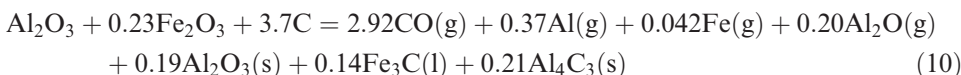


Table 1. Bauxite specifications, weight percent, for dried Jamaican type, African Gold Coast, British Guyana, Greek, Western Australian, Weipa Range Australian (from Totten and MacKenzie 2007), and Russian (Goldin et al. 1998) bauxite. The wt.% compositions are for the major components only

Composition Wt.%	Jamaican type	African Gold Coast	British Guyana	Greek	Western Australia	Weipa Australia	Russian
Al_2O_3	47.0	55.2	61.1	60.2	30–35	57.0	75.3
SiO_2	3.0	2.0	5.0	3.1	2.0	5.0	15.3
Fe_2O_3	22.0	11.5	1.5	21.7	20.0	7.5	2.9
TiO_2	3.0	2.1	2.5	3.0		2.5	4.6

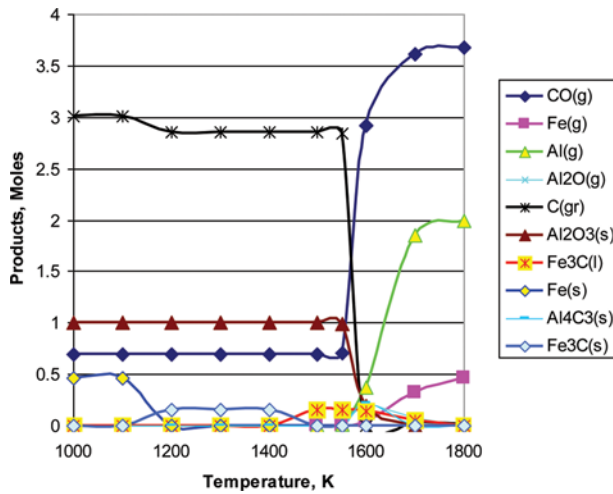


Figure 8 Temperature dependence for the system $\text{Al}_2\text{O}_3 + 0.23\text{Fe}_2\text{O}_3 + 3.7\text{C}$ at 10^{-4} bar (color figure available online).

At 1500 K and 10^{-5} bar, the equilibrium formed is:

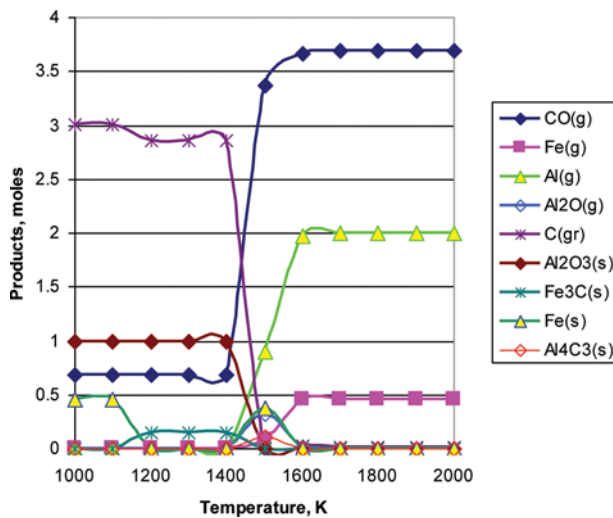
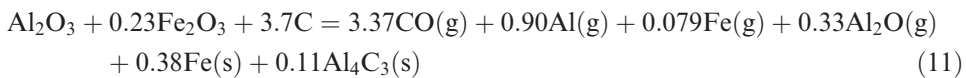


Figure 9 Temperature dependence for the system $\text{Al}_2\text{O}_3 + 0.23\text{Fe}_2\text{O}_3 + 3.7\text{C}$ at 10^{-5} bar (color figure available online).

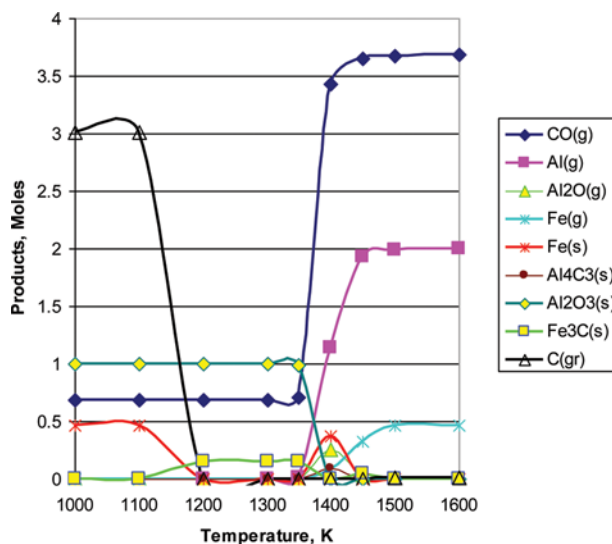
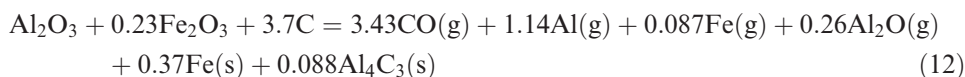


Figure 10 Temperature dependence for the system $\text{Al}_2\text{O}_3 + 0.23\text{Fe}_2\text{O}_3 + 3.7\text{C}$ at 10^{-6} bar (color figure available online).

At 1400 K and 10^{-6} bar, the equilibrium formed is:



The resulting $\text{Fe}(\text{g})/\text{Al}(\text{g})$ atomic ratios at those temperatures are summarized in Table 2. As shown in the Table, better separation of iron from aluminum is expected at lower vacuum pressure and lower temperature.

DISCUSSION AND CONCLUSIONS

The equilibrium calculations indicate the possibility of releasing gaseous aluminum directly by vacuum carbothermic reduction of iron-free bauxite at 1400–1500 K and 10^{-7} bar. A more moderate vacuum could be applied at a higher reaction temperature. Energetic and environmental assessments of the proposed process are presented in Tables 3 and 4 for the reactions of $\text{AlO}(\text{OH})$ or $\text{Al}(\text{OH})_3$ in the presence

Table 2. Temperatures at which small $\text{Fe}(\text{g})/\text{Al}(\text{g})$ atomic ratios are expected for the system $\text{Al}_2\text{O}_3 + 0.23\text{Fe}_2\text{O}_3 + 3.7\text{C}$ at 10^{-4} , 10^{-5} , and 10^{-6} bar

Pressure, bar	Temperature, K	$\text{Fe}(\text{g})/\text{Al}(\text{g})$ atomic ratio
10^{-4}	1600	0.114
10^{-5}	1500	0.087
10^{-6}	1400	0.076

Table 3. Environmental assessment for the vacuum carbothermal reduction of an initial mixture of $\text{AlO}(\text{OH}) + 0.2\text{SiO}_2 + 2.4\text{C}$ at 10^{-7} bar reaching at 1400 K the equilibrium composition of $2.30\text{CO}(\text{g}) + 0.99\text{Al}(\text{g}) + 0.48\text{H}_2(\text{g}) + 0.10\text{SiO}(\text{g}) + 0.1\text{SiC}(\text{s})$. By partial WGS (water-gas shift) of CO to H_2 , a syngas of molar ratio $\text{H}_2/\text{CO} = 2$ is proposed to be obtained, and converted to methanol

Design parameters	
AlO(OH) feed (kmol) ¹	1
SiO ₂ feed (kmol/kmol Al)	0.2
Coke feed (kmol/kmol Al)	2.4
Coke feed (GJ/kmol Al) ²	0.944
Heat and Work input	
Process heat (GJ/kmol Al) ³	0.895
Pumping work (GJ/kmol Al) ⁴	0.738
Theoretical heat & work (GJ/kg Al)	0.060
CO₂ release & methanol production	
Calculated CO ₂ release (kmol/kg Al) ⁵	0.152
Calculated CO ₂ release (kg/kg Al)	6.71
WGS CO ₂ release (kmol/kmol Al) ⁶	1.4
WGS CO ₂ release (kg/kg Al)	2.24
Total CO ₂ release (kg/kg Al) ⁵	8.95
Total CO ₂ release (kg/kg Al) ⁷	5.26
Methanol production (kmol/kmol Al) ⁸	0.81
Methanol production (kg/kg Al)	0.96

¹AlO(OH), boehmite or diaspore minerals.

²Taking the HHV of graphite, 393.5 kJ/mol, as representative of coke.

³Theoretical process heat for changing equilibrium composition from 300 to 1400 K at 1 bar.

⁴Theoretical work for isothermal expansion at 1400 K of product gases from 1 bar to 10^{-7} bar.

⁵Assume fossil fuel both for process heat and for electricity generation.

⁶From partial WGS of CO to H_2 to produce syngas.

⁷Assume process heat supplied by concentrated solar energy.

⁸Assume 90% chemical yield of methanol from syngas.

of SiO_2 . The carbon reducing agent could be charcoal, coke, petcoke, or other carbon sources. Also, the conversion of the released carbon monoxide via syngas to methanol is shown as an example of the utilization of the CO- H_2 mixture. Other products from syngas such as hydrocarbons, hydrogen, and ammonia are feasible and would contribute to the process economics. Alternatively, syngas coproduced may be used as combustion fuel for power generation. The presence of noncondensable gas considerably reduces the level of condensation heat transfer. The condensation of aluminum vapors and its separation in liquid phase from its mixture with CO on a cold surface under low pressure presents a diffusional resistance due to the fact that the CO tends to collect near the cold surface. This difficulty can be overcome by condensation in direct contact between the Al vapors and the liquid phase Al through bubbling or in a similar mechanism as occurs in a distillation column. The total theoretical process heat and work requirement from AlO(OH) would amount to about 0.06 GJ/kg Al. Using the released CO for the coproduction (via syngas) of 0.96 kg methanol/kg Al would result in an overall specific CO₂ emission of about 8.95 kg CO₂/kg Al. With concentrated solar energy for process heat, the coproduction of methanol would result in specific emission of about 5.26 kg CO₂/kg Al (Table 3). By a similar calculation for the reaction from $\text{Al}(\text{OH})_3$, the total

Table 4. Environmental assessment for the vacuum carbothermal reduction of an initial mixture of $\text{Al}(\text{OH})_3 + 0.2\text{SiO}_2 + 3.4\text{C}$ at 10^{-7} bar reaching at 1400 K the equilibrium composition of $3.30\text{CO}(\text{g}) + 0.99\text{Al}(\text{g}) + 1.48\text{H}_2(\text{g}) + 0.10\text{SiO}(\text{g}) + 0.1\text{SiC}(\text{s})$. By partial WGS (water-gas shift) of CO to H_2 , a syngas of molar ratio $\text{H}_2/\text{CO} = 2$ may be obtained, and converted to methanol

Design parameters	
Al(OH) ₃ feed (kmol) ¹	1
SiO ₂ feed (kmol/kmol Al)	0.2
Coke feed (kmol/kmol Al)	3.4
Coke feed (GJ/kmol Al) ²	1.338
Heat and Work input	
Process heat (GJ/kmol Al) ³	1.14
Pumping work (GJ/kmol Al) ⁴	1.12
Theoretical heat & work (GJ/kg Al)	0.083
CO₂ release & methanol production	
Calculated CO ₂ release (kmol/kg Al) ⁵	0.211
Calculated CO ₂ release (kg/kg Al)	9.28
WGS CO ₂ release (kmol/kmol Al) ⁶	1.2
WGS CO ₂ release (kg/kg Al)	1.96
Total CO ₂ release (kg/kg Al) ⁵	11.24
Total CO ₂ release (kg/kg Al) ⁷	6.60
Methanol production (kmol/kmol Al) ⁸	1.42
Methanol production (kg/kg Al)	1.69

¹Al(OH)₃, gibbsite mineral.

²Taking the HHV of graphite, 393.5 kJ/mol, as representative of coke.

³Theoretical process heat for changing equilibrium composition from 300 to 1400 K at 1 bar.

⁴Theoretical work for isothermal expansion at 1400 K of product gases from 1 bar to 10^{-7} bar.

⁵Assume fossil fuel combustion both for process heat and for electricity generation.

⁶From partial WGS of CO to H_2 for syngas production.

⁷Assume process heat supplied by concentrated solar energy.

⁸Assume 90% chemical yield of methanol from syngas.

theoretical process heat and work requirement would amount to about 0.083 GJ/kg Al (Table 4). Assuming the coproduction via syngas of 1.69 kg methanol/kg Al would result in an overall specific CO₂ emission of about 11 kg CO₂/kg Al. With concentrated solar process heat, the coproduction of methanol would result in about 6.6 kg CO₂/kg Al.

In modern Bayer process plants, 208 kg bauxite yield on average 75.9 kg Al₂O₃, or 140 kg bauxite/kmol Al, and have a total energy requirement—usually supplied by fossil fuel burning—of 0.012 GJ/kg alumina produced, or 0.023 GJ/kg Al (International Aluminum Institute, 2009). In modern Hall-Héroult process plants, 15.2 MWhr are required per metric ton Al produced, or 0.045 GJ/kg Al. The total energy demand in modern primary Al production from bauxite by the above two processes is thus 0.068 GJ/kg Al. Mining, transportation, crushing of the minerals, disposal of the Bayer process wastes (red mud), and the transportation of materials further raises considerably the total energy demand. A “cradle-to-gate” life cycle assessment indicates that the gross energy requirement (GER) of current primary aluminum production is 0.211 GJ/kg Al, and the global warming potential (GWP) is 22.4 kg CO₂equiv/kg Al (Norgate, Jahanshahi, and Rankin 2007). The proposed process of direct vacuum carbothermic reduction of iron-free bauxite to aluminum could

possibly result in significant reduction of greenhouse gas emission, avoidance of “red mud” production, and fuel savings. For iron-rich bauxite, one option would be to first remove most of the iron (Reddy, Mishra, and Banerjee 1999; Gülfen, Gülfen, and Ayden 2006; Renata et al. 2009). As shown in Figures. 6–10 for the carbothermal reduction, at about 1000–1100 K the iron oxide is completely reduced to Fe(s), while alumina remains unchanged. These conditions could perhaps enable the removal of iron from alumina, e.g., by magnetic separation. In addition, as shown in Table 3, the equilibrium calculations indicate that under specific temperature and vacuum pressure conditions, Al(g) may be selectively produced relative to Fe(g). This still needs to be confirmed experimentally. Further study will be required also to test the selectivity of the process to minor metals in bauxite. An alternative approach to the carbothermal reduction of alumina has been in molten Sn or Cu at pressures 0.08–0.20 bar and in the temperature range 1700–1850°C, with the Al formed remaining in the alloy phase (Frank, Finn, and Elliott 1989). It may be difficult to extract pure Al from the alloy but such a method could be useful for producing certain alloys. The direct carbothermic reduction on the hydrated forms of bauxite, i.e., AlO(OH) and Al(OH)₃ rather than on Al₂O₃ could be advantageous, as it would save the energy cost of the separate step of calcination, and would yield a CO-H₂ mixture useful as combustion fuel, or for the production of syngas.

ACKNOWLEDGMENT

The authors acknowledge the financial support of EU-project ENEXAL.

REFERENCES

- Aluminum of Greece. www.alhellas.gr.
- Choate, W. T. and Green, J. A. S., 2006, “Technoeconomic assessment of the carbothermic reduction process for aluminum production,” *Light Metals*, pp. 445–450. See also: Choate, W. T., and Green, J. A. S., 2003, “U.S. Energy Requirements for Aluminum Production, Historical Perspective, Theoretical Limits and New Opportunities.” http://www1.eere.energy.gov/industry/aluminum/pdfs/al_theoretical.pdf.
- FactSage, Thermochemical Software & Database Package, Centre for Research in Computational Thermochemistry, Ecole Polytechnique de Montreal, Canada. <http://www.crcr.polymtl.ca>.
- Frank, R. A., Finn, C. W., and Elliott, J. F., 1989, “Physical chemistry of the carbothermic reduction of alumina in the presence of a metallic solvent. Part II. Measurement of the kinetics of reaction,” *Metallurgical Transactions B-Process Metallurgy*, 20, pp. 161–173.
- Goldin, B. A., Grass, V. E., and Ryabkov, Yu. I., 1998, “Vacuum carboprocessing of low-iron bauxites,” *Glass and Ceramics*, 55(9–10), pp. 323–325.
- Gülfen, G., Gülfen, M., and Ayden, A. O., 2006, “Dissolution kinetics of iron from diasporic bauxite in hydrochloric acid solution,” *Indian Journal of Chemical Technology*, 13, pp. 386–390.
- Halmann, M., Frei, A., and Steinfeld, A., 2007, “Carbothermal reduction of alumina, Thermochemical equilibrium calculations and experimental investigation,” *Energy*, 32, pp. 2420–2427.
- International Aluminum Institute, Aluminum for Future Generations/2009 Update. <http://www.world-aluminium.org.pdf>. Accessed December 7, 2011.

- Kruesi, M., Galvez, M. E., Halmann, M., Steinfeld, A., 2011, "Solar aluminum production by vacuum carbothermal reduction of alumina—Thermodynamic and experimental analyses," *Metallurgical and Materials Transactions B*, 42B, pp. 254–260.
- Murray, J. P., 1999, "Aluminum production using high-temperature solar process heat," *Solar Energy*, 66, pp. 133–142.
- Murray, J. P., 2001, "Solar production of aluminum by direct reduction of ore to Al-Si alloy. Preliminary results for two processes," *Journal of Solar Energy Engineering*, 123, pp. 125–132.
- Murray, J. P., Steinfeld, A., and Fletcher, E. A., 1995, "Metals, nitrides, and carbides via solar carbothermal reduction of metal oxides," *Energy*, 20, pp. 695–704.
- NIST, National Institute of Standards and Technology, Standard Reference Data Program, Chemistry Webbook. <http://webbook.nist.gov/chemistry>.
- Norgate, T. E., Jahanshahi, S., and Rankin, W. J., 2007, "Assessing the environmental impact of metal production processes," *Journal of Cleaner Production*, 15, pp. 838–848.
- Reddy, B. R., Mishra, S. K., and Banerjee, G. N., 1999, "Kinetics of leaching of a gibbsitic bauxite with hydrochloric acid," *Hydrometallurgy*, 51, pp. 131–138.
- Renata, S. K., Arthur, P. C., Christian, F. de A., and Claret, A. V. A., 2009, "Concentration of bauxite fines via froth flotation," *Revista Escola de Minas*, 62, pp. 271–276.
- Totten, G. E. and MacKenzie, D. S., 2007, *Handbook of Aluminum*, Boston: Academic Press.
- Yang, D., Feng, N.-X., Wang, Y.-W., Wu, X.-L., 2010, "Preparation of primary Al-Si alloy from bauxite tailings by carbothermal reduction process," *Trans. Nonferrous Metals Soc. China*, 20, pp. 147–152.